Functions and regulation of the Nox family in the filamentous fungus *Podospora anserina*: a new role in cellulose degradation

Sylvain Brun,[1,2] **Fabienne Malagnac,**[1,2] **Frédérique Bidard,**[2] **Hervé Lalucque**[1,2] **and Philippe Silar**[1,2]*

[1]*UFR des Sciences du Vivant, Univ Paris 7 Denis Diderot, 75005 Paris, France.*

[2]*Institut de Génétique et Microbiologie, UMR CNRS 8621, Univ Paris Sud 11, 91405 Orsay cedex, France.*

Summary

NADPH oxidases are enzymes that produce reactive oxygen species. Studies in mammals, plants and fungi have shown that they play important roles in differentiation, defence, host/pathogen interaction and mutualistic symbiosis. In this paper, we have identified a *Podospora anserina* mutant strain impaired for processes controlled by PaNox1 and PaNox2, the two Nox isoforms characterized in this model ascomycete. We show that the gene mutated is *PaNoxR*, the homologue of the gene encoding the regulatory subunit p67[phox]**, conserved in mammals and fungi, and that PaNoxR regulates both PaNox1 and PaNox2. Genome sequence analysis of *P. anserina* reveals that this fungus posses a third Nox isoform, PaNox3, related to human Nox5/Duox and plant Rboh. We have generated a knock-out mutant of *PaNox3* and report that PaNox3 plays a minor role in *P. anserina*, if any. We show that PaNox1 and PaNox2 play antagonist roles in cellulose degradation. Finally, we report for the first time that a saprobic fungus, *P. anserina*, develops special cell structures dedicated to breach and to exploit a solid cellulosic substrate, cellophane. Importantly, as for similar structures present in some plant pathogens, their proper differentiation requires PaNox1, PaNox2, PaNoxR and the tetraspanin PaPls1.**

Introduction

Reactive oxygen species (ROS) have for a long time been considered as deleterious by-products of aerobic metabolism. However, studies on NADPH oxidases (Nox), a large family of enzymes dedicated to ROS production, have recently shed light on the many important biological roles of ROS. Nox are enzymes of the plasma membrane that utilize NADPH to generate superoxide ($O2^-$). Absent in prokaryotes, Nox are present in a large array of mainly multicellular eukaryotes (Lalucque and Silar, 2003). We have proposed that the ancestral role of Nox-mediated ROS production in Eukaryota might have been cell-to-cell communication by informing its neighbours of the nutritional status of the cell (Lalucque and Silar, 2003). Accordingly, Nox enzymes are now involved in regulating the development of multicellular structures that involve interactions of cells from the same species or in modulating symbiosis in which cells of different species interact. Studies on two of the fungal Nox emphasize both roles (for reviews see Aguirre *et al.*, 2005; Takemoto *et al.*, 2007).

First, Nox1 (also known as NoxA) controls the building of the multicellular fruiting body in *Neurospora crassa*, *Aspergillus nidulans* and *Podospora anserina* (Lara-Ortiz *et al.*, 2003; Malagnac *et al.*, 2004; Cano-Dominguez *et al.*, 2008); in the plant pathogens *Botrytis cinerea* and *Claviceps purpurea*, Nox1 is involved in sclerotia formation, small multicellular structures involved in long-term survival (Giesbert *et al.*, 2008; Segmuller *et al.*, 2008). The Nox1 enzyme is present in a large range of fungi but is absent from many species unable to build multicellular fructification, including Saccharomycotina, Taphrinomycotina and Agaricomycotina yeasts (Lalucque and Silar, 2003; Takemoto *et al.*, 2007). The Nox2 (or NoxB) enzyme is present in a more restricted set of fungi than Nox1, as it is, for example, not found in Eurotiomycetes and some Dothideomycetes (Lalucque and Silar, 2003; Takemoto *et al.*, 2007). It is required for ascospore germination in *P. anserina* and *N. crassa* (Malagnac *et al.*, 2004; Cano-Dominguez *et al.*, 2008). Recently, we described an additional role for this enzyme in nutrient acquisition when grown on media containing paper as

carbon source. This impacts on the number and the rep-artition of fruiting bodies on the thallus (Malagnac *et al.*, 2008).

Second, fungal Nox play important functions in parasitic and mutualistic symbiosis. In *P. anserina*, Nox1 (but not Nox2) plays a major role in hyphal interference, a contact defence mechanism towards fungal competitors (Silar, 2005). In the hemi-biotrophic rice pathogen *Magnaporthe grisea*, both Nox1 and Nox2 are required in appressorium to breach the cuticle of the host plant (Egan *et al.*, 2007). In addition, both *Nox1* and *Nox2* null mutants are unable to grow *in planta*, even when allowed to penetrate through a wound (Egan *et al.*, 2007). In the necrotrophic plant pathogen *B. cinerea*, *Nox1* and *Nox2* act at different steps of pathogenesis. While *Nox2* is required in the appressorium-like structure that enables the fungus to penetrate its hosts, *Nox1* is necessary for subsequent growth *in planta* (Segmuller *et al.*, 2008). In *C. purpurea*, *Nox1* is also necessary for growth *in planta* (Giesbert *et al.*, 2008). On the contrary, growth of *NoxA* mutants of the mutualistic fungus *Epichloë festucae* in the perennial ryegrass is anarchic and invasive, leading to increased fungal biomass that provokes loss of symbiosis and premature senescence of the host (Tanaka *et al.*, 2006).

Fungal Nox1 and Nox2 are very similar enzymes and the different roles they exert address the question of the specific regulation of the two isoforms during the life cycle of the fungus. In plants and mammals, Nox enzymes are mainly regulated post-transcriptionally by recruitment of additional regulatory subunits with the core enzyme on the one hand (mammalian Nox1 to Nox4) or by calcium on the other hand (mammalian Nox5 and plant Rboh). The best-characterized member of this group of enzymes is Nox2/gp91^{phox}, which is responsible for the phagocytic 'oxidative burst', a hallmark of the mammalian innate immune response towards invading microbes (see Sumimoto, 2008 for a review). The redox core of the oxidase is the membrane-spanning flavocytochrome b_{558} comprising the catalytic subunit gp91^{phox} and its adaptator p22^{phox}. Upon cell stimulation, flavocytochrome b_{558} is activated by recruitment of four cytosolic components, namely p40^{phox}, p47^{phox}, p67^{phox} and the Rho-type G-protein Rac. In humans, defects in any of the four genes *p22^{phox}*, *p40^{phox}*, *p47^{phox}* and *p67^{phox}* cause primary immunodeficiency chronic granulomatous disease, as do mutations in *gp91^{phox}*. Similar activation has been found for the Nox1 isoform for which p47^{phox} and p67^{phox} are replaced by their respective paralogues NOXO1 and NOXA1 in the regulatory complex. In fungi, sequence analyses of the many genomes available solely identified homologues of p67^{phox}, called NoxR and homologues of Rac (Takemoto *et al.*, 2006; Takemoto *et al.*, 2007). Functional studies of NoxR (in *E. festucae*, *B. cinerea* and *N. crassa*) and Rac (in *E. festucae* and *M. grisea*) point to the evolutionary

conservation of Nox activation by both NoxR and Rac (Takemoto *et al.*, 2006; Cano-Dominguez *et al.*, 2008; Chen *et al.*, 2008; Segmuller *et al.*, 2008). In *B. cinerea* and *N. crassa*, deletion of NoxR indicates that this regulatory subunit is required for both Nox1 and Nox2 functions (Cano-Dominguez *et al.*, 2008; Segmuller *et al.*, 2008). In contrast, in *E. festucae*, NoxR may not be required for NoxA function *in vitro* and its role in regulating NoxB remains unknown (Takemoto *et al.*, 2006). How Nox isoforms exert different biological roles in fungi, despite having the same enzymatic activity, remains to be explored.

The coprophilous fungus *P. anserina* is a powerful model amenable for extensive genetic screens and studies. The *IDC^{343}* mutant that is impaired for the *PaNox1* gene was recovered in a screen designed to uncover genes involved in Crippled Growth (CG; Malagnac *et al.*, 2004; Haedens *et al.*, 2005). CG corresponds to a cell degeneration phenomenon controlled epigenetically by an inheritable and infectious factor resembling a prion (Silar *et al.*, 1999; Kicka *et al.*, 2006). In addition to PaNox1, this genetic screen led to the identification of the MAP kinase kinase kinase (MAPKKK) PaASK1, the MAP kinase kinase (MAPKK) PaMKK1 and of the pezizomy-cota specific gene *IDC1* (Kicka and Silar, 2004; Malagnac *et al.*, 2004; Haedens *et al.*, 2005; Kicka *et al.*, 2006; Jamet-Vierny *et al.*, 2007). We have shown that *PaNox1* and *IDC1* act on the PaASK1/PaMKK1/PaMpk1 MAPK-module by promoting nuclear translocation of the PaMpk1 MAP kinase (Malagnac *et al.*, 2004; Kicka *et al.*, 2006; Jamet-Vierny *et al.*, 2007). We now report the characterization of the *IDC^{524}* mutant obtained in the same genetic screen (Haedens *et al.*, 2005) and show that the gene mutated in *IDC^{524}* is the *P. anserina* p67^{phox} homologue, *PaNoxR*. We also show a conservation of the regulatory role of PaNoxR towards both Nox isoforms PaNox1 and PaNox2 in *P. anserina*. The entire genome of *P. anserina* has been recently sequenced (Espagne *et al.*, 2008) and careful analysis has identified a third isoform belonging to the Nox3/NoxC family, PaNox3. As for human Nox5 and Duox, and plant Rboh, Nox enzymes of this subfamily bear EF-hand calcium binding motifs. Accordingly, calcium regulates human Nox5, Duox and plant Rboh (Sumimoto, 2008). In view of characterizing the role of the Nox3 isoform in the physiology of fungi, we have generated the K.O. strain for *PaNox3*, *ΔPaNox3*. We report here that calcium has no effect on *PaNox3* mutants and that PaNox3 plays a minor role in *P. anserina*, at least in laboratory conditions.

The exact function(s) of ROS and the role of Nox in fungi are still not fully understood and are sometimes puzzling. In particular, loss-of-function of *Nox* genes can seemingly lead to increased ROS production. In *P. anserina*, previous analysis of mutants inactivated for

PaNox1 or for both *PaNox1* and *PaNox2* (*PaNox1,2* mutants) revealed greatly enhanced staining by both diaminobenzidine (DAB) and nitroblue tetrazolium (NBT), two classical assays performed to detect peroxide and superoxide ions respectively (Malagnac *et al.*, 2004). We show here that this enhanced redox activity is correlated with enhanced capacity to degrade cellulose in strains lacking PaNox1. Transcriptomic analysis of the *PaNox1* null mutant confirmed that the genes involved in cellulose degradation were upregulated in this strain. Moreover, visualization of cellulose utilization at the cellular level revealed that the saprobic *P. anserina* attacks cellophane by making special cell structures able to penetrate and to breach cellophane. Strikingly, as for appressorium in plant pathogens such as *M. grisea* and *B. cinerea*, the proper differentiation of these structures requires PaNox1, PaNox2, PaNoxR and the PaPls1 tetraspanin.

Results

Mutations in PaNoxR *recapitulate the phenotypes of the* PaNox1,2 *double mutants*

Among all the mutants screened during the search for the suppressor of CG, *IDC*[524] was of great interest. Indeed, *IDC*[524] displayed the same pigment, aerial hyphae, fertility and lack of CG defaults as the *PaNox1* mutant *IDC*[343], and in addition, *IDC*[524] ascospores germinated as poorly as the *ΔPaNox2* ascospores (Haedens *et al.*, 2005). Thus, *IDC*[524] seemed to combine the phenotypes of the *PaNox1* and *PaNox2* mutants, as do the *PaNox1,2* double mutants. Interestingly, genetic mapping indicated that the mutated gene was located at the centromere of chromosome 7 of *P. anserina*, a location where an ortho-logue of the gene encoding mammalian p67[phox] is located. Indeed, a search of the complete *P. anserina* genome (available at http://podospora.igmors.u-psud.fr; Espagne *et al.*, 2008) by BLAST with *Mus musculus* p22[phox], p40[phox] or p47[phox] as query, revealed that it does not encode a clear homologue for these three factors as previously reported (Takemoto *et al.*, 2007). However, a putative homologue of p67[phox] was uncovered (Fig. S1), as described for other fungi (Takemoto *et al.*, 2007). The CDS Pa_7_11300 encoding this putative p67[phox] homo-logue was called PaNoxR. Two Expressed Sequenced Tags covering *PaNoxR* were present in the database (Espagne *et al.*, 2008), validating the predicted annotation and indicating that it was expressed. Microarray data showed that *PaNoxR* was transcribed throughout the life cycle, as are *PaNox1* and *PaNox2* (F. Bidard, unpubl. data). To test if *IDC*[524] is mutated in *PaNoxR*, it was co-transformed with a PCR DNA fragment encompassing the Pa_7_11300 CDS and a plasmid conferring resistance to phleomycin. Among the 23 phleomycin resistant trans-

formants recovered, two showed partial phenotype recov-ery, while two others displayed a wild-type phenotype. These data suggested that *PaNoxR* was the gene affected in *IDC*[524]. To verify this, *PaNoxR* was amplified by PCR from the *IDC*[524] mutant. Sequence analysis of three independent PCR products revealed that the muta-tion in *IDC*[524] was a T to C transition in the CDS, changing a leucine to a proline at position 14 of the encoded protein (Fig. S1).

Since *IDC*[524] may not be a null allele, *PaNoxR* was deleted by gene replacement in a *Δmus51* strain, which exhibits improved homologous recombination (El-Khoury *et al.*, 2008). The *ΔPaNoxR Δmus51* deleted strains were then crossed with wild-type to outcross the *Δmus51* mutation (see *Experimental procedures* for mutant construction). Phenotypes of *ΔPaNoxR* and *IDC*[524] mutants were evaluated throughout the life cycle (Fig. 1). Both strictly recapitulated the phenotype exhibited by the inactivation of *PaNox1* and *PaNox2*. *IDC*[524] and *ΔPaNoxR* ascospores germinated as poorly as the *ΔPaNox2* null mutant (Fig. 1A). They had the same myce-lium morphology, behaviour towards CG (Fig. 1B) and hyphal interference (Fig. 1C) as the *PaNox1* null mutant *IDC*[343]. *IDC*[524] and *ΔPaNoxR* differentiated ascogonia, but were unable to mate as female in crosses as *IDC*[343]. Mosaic analysis, as previously performed (Jamet-Vierny *et al.*, 2007), indicated that PaNoxR was required in the envelope of the developing fructification (Fig. 1D), as is PaNox1. Moreover, fertility of *ΔPaNoxR* was not restored by transfer to fresh media and both DAB and NBT staining were enhanced in the *ΔPaNoxR* strains compared with *IDC*[343] (Fig. 2), two phenotypes of the *PaNox1,2* double mutants (Malagnac *et al.*, 2004). DAB and NBT staining are classical assays to detect peroxide and superoxide respectively (Munkres, 1990). Therefore, enhanced stain-ing in *IDC*[343], *PaNox1,2* and *ΔPaNoxR* mutants sug-gested that another source of ROS is present in these strains and that this source is upregulated in the absence of Nox1 and Nox2. Interestingly, the *P. anserina* genome contains a third Nox isoform that belongs to the Nox3/NoxC family (CDS Pa_1_5020), PaNox3. Yet, the role of Nox3 remains unknown in fungi and PaNox3 is a good candidate as alternative source of ROS in *P. anserina*.

Nox 3 is frequently lost in fungi and the PaNox3 *mutant presents no phenotype in laboratory conditions*

PaNox3, the enzyme encoded by Pa_1_5020 carries one EF-hand calcium-binding motif (Fig. S2), as described for other enzymes of the Nox3/NoxC subfamily (Aguirre *et al.*, 2005). Although no EST for *PaNox3* was present in the database (Espagne *et al.*, 2008), microarray analyses showed that *PaNox3* was expressed throughout the life cycle (F. Bidard, unpubl. data). The Nox3 isoform presents
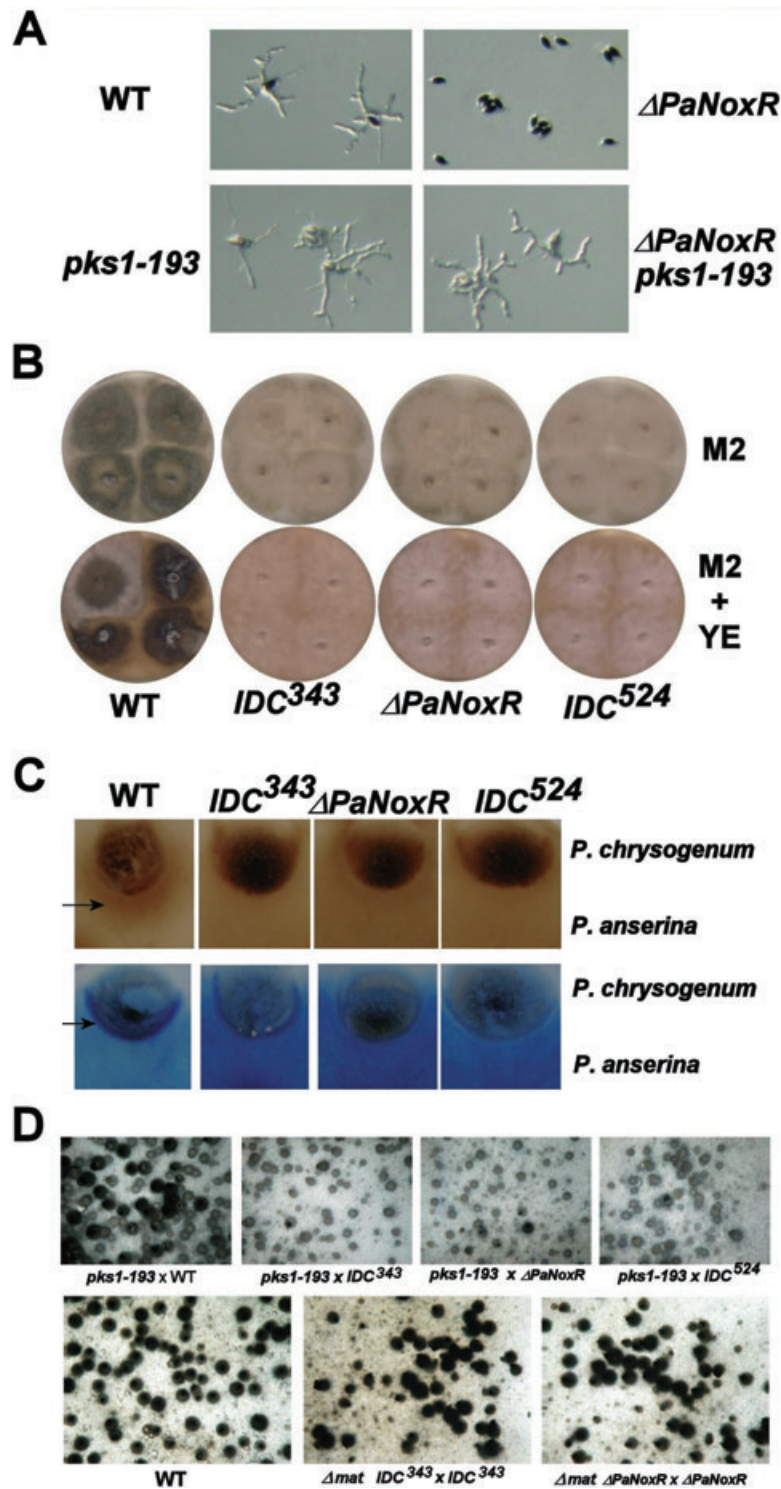
a patchy phylogenetic repartition in fungal species (Takemoto *et al.*, 2007). It is presently encountered in 11 ascomycetes from different clades. Nox3 evolution follows the known relationships of fungal phylogeny (Hibbett *et al.*, 2007), with very high statistical support (Fig. 3), indicating that no horizontal transfer has occurred between distant species. Interestingly, in *Mycosphaerella fijiensis*, the putative Nox3 gene is interrupted by a frameshift (Fig. S3). The patchy repartition observed is thus likely due to recurrent losses of *Nox3* genes. Finally, Nox3 exhibits a higher evolution rate than the Nox1/NoxA and Nox2/NoxB isoforms (Table S1). Overall, these data

Fig. 1. Phenotypes of the *ΔPaNoxR* and *IDC^524* mutants.

A. *mat+/mat–* heterokaryotic ascospores of the indicated genotypes were recovered on germination media and incubated for 6 h. *ΔPaNoxR* ascospores germinate very poorly (top right) at a rate of about 1 out of 10 000 as described for the *ΔPaNox2* mutant (Malagnac *et al.*, 2004). Further incubation does not result in germination of *ΔPaNoxR* ascospores. The *ΔPaNoxR* germination defect is identical to that of *ΔPaNox2* (Malagnac *et al.*, 2004; Lambou *et al.*, 2008), since it is ascospore autonomous, *ΔPaNoxR* ascospores do not form the germination peg, and removal of melanin from *ΔPaNoxR* ascospores, either by adding the *pks1–193* mutation (bottom right) or by adding tricyclazole in the medium (Coppin and Silar, 2007), permits a 50% germination rate. WT, wild-type.

B. Homokaryotic strains were inoculated on M2 and M2 + 5 g l⁻¹ of yeast extract (M2 + YE) to test mycelium morphology as well as Crippled Growth (CG), as previously described (Haedens *et al.*, 2005). On M2 medium, wild-type (WT) presents aerial hyphae, accumulates melanin and does not display CG. On this medium, the *IDC^343*, *IDC^524* and *ΔPaNoxR* mutants grow at the same rate as wild-type and produce a dense network of hyphae. However, they do not accumulate pigment, lack aerial hyphae and are sterile (they nonetheless differentiate male gametes and female gametangia). On M2 + YE, wild-type exhibits CG, which is visible as darkly pigmented thalli; the top left mycelia of the Petri plate being in Normal Growing state. On the contrary, *IDC^343*, *IDC^524* and *ΔPaNoxR* mycelia do not degenerate by CG.

C. Hyphal Interference against *Penicillium chrysogenum* was assayed after 2 days of contact. Top row illustrates lack of oxidative burst in the *IDC^343*, *IDC^524* and *ΔPaNoxR* mutants after they contact *P. chrysogenum*. The burst (arrow) is visible in the case of contact with wild-type *P. anserina*. Bottom row illustrates the diminished accumulation of dead *P. chrysogenum* hyphae when confronted with *P. anserina* mutants, as compared with confrontation with the wild-type strain (arrow). See Silar (2005) for further details.

D. Female sterility of *ΔPaNoxR* and *IDC^524* is due to the inability to build the perithecium envelope. In *P. anserina*, fertilization triggers the development of multicellular fructification (perithecium), whose envelope is only of maternal origin. Observation of perithecia formed by the indicated heterokaryons was made after 7 days of incubation. Unlike what is observed for wild-type, crossing the mutants with *pks1–193* yields essentially non-pigmented perithecia originating from the *pks1–193* parent indicating that the genes affected in the mutants are necessary in the female partner of the cross. Recovery of perithecium production in the *Δmat/IDC^343 mat+/IDC^343 mat–* and *Δmat/ΔPaNoxR mat+/ΔPaNoxR mat–* trikaryons indicates that PaNox1 and PaNoxR are required specifically in the envelope. See (Jamet-Vierny *et al.*, 2007) for further information.

suggest that the evolutionary constraint on the Nox3 isoform is less than that on the Nox1 and Nox2 isoforms.

With the aim to functionally test *PaNox3*, the *PaNox3* coding sequence was deleted (see *Experimental procedures* for mutant construction). No phenotype modifica-

tion was detected for the *ΔPaNox3* mutant with regard to ascospore germination, mycelium morphology, growth rate (at four different temperatures and on media with varying concentrations of nutrients), longevity, ability to perform anastomoses, CG and hyphal interference. No
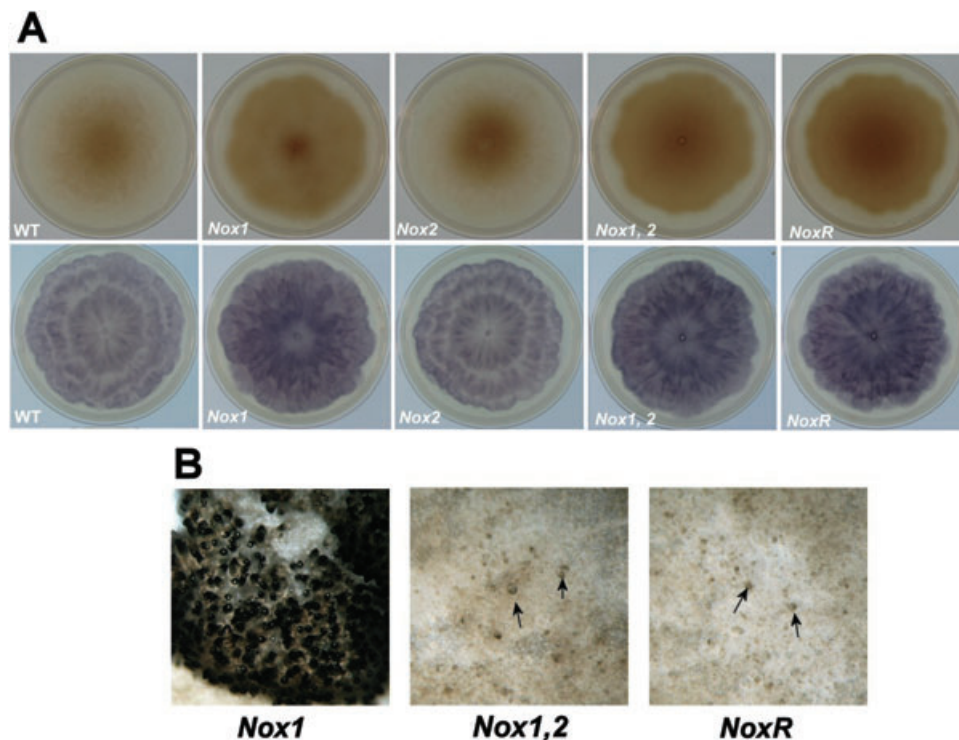
Fig. 2. Comparison of the *ΔPaNoxR* phenotypes with that of the *PaNox1,2* double mutant.

A. DAB reduction (Top row) and NBT reduction (bottom row) were assayed on 6-day-old cultures of strains carrying the *pks1–193* allele and the indicated null alleles of *PaNox1*, *PaNox2* and *PaNoxR*.

B. Restoration of perithecium production was assayed by transferring *IDC^343* (*Nox1*), *ΔPaNox2* (*Nox2*) and *ΔPaNoxR* (*NoxR*) crosses set up on cellophane on fresh medium as described (Malagnac *et al.*, 2004). Large and ascospore-containing perithecia are observed with *IDC^343* (*Nox1*) whereas tiny abortive fructifications (arrows) are recovered with *ΔPaNoxR* (*NoxR*) and *PaNox1,2* (*Nox1,2*).
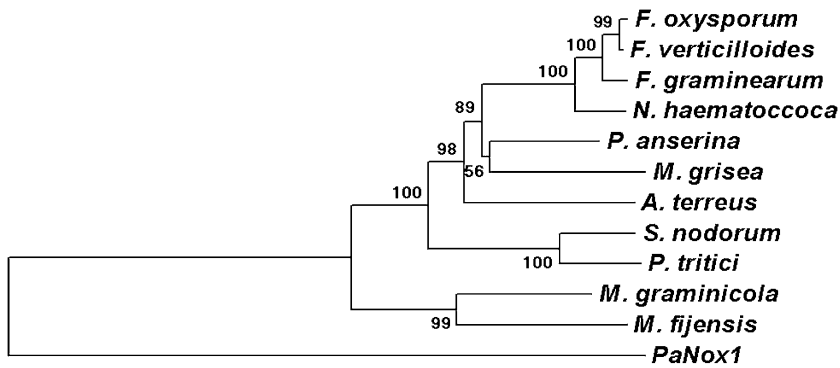
Fig. 3. Neighbour-Joining phylogenetic tree of fungal Nox3/NoxC isoforms. The protein sequences were aligned using the MAFFT program with the default parameters (see Fig. S3; Katoh *et al.*, 2005) and phylogenetic trees were generated using MEGA4 with the default parameters (Tamura *et al.*, 2007). The tree was rooted with the PaNox1 sequence and tested by 1000 replica of bootstrap. Trees with identical topology were recovered using the minimum evolution and maximum parsimony methods.

modification of DAB and NBT staining was observed (Fig. S4). We also did not detect any modification of fertility in confrontation crosses or as heterokaryons at four different temperatures (18°C, 27°C, 30°C and 37°C) on dextrin-containing medium, nor did we see any growth or fertility modification on media containing alternative carbon sources such as glucose, paper, cellophane or cellulose powder.

Because PaNox3 contains putative calcium binding sites, we investigated the effects of excess and deprivation of Ca^{2+} on growth and fertility of wild-type and *ΔPaNox3* in medium with dextrin or with paper as carbon source. Wild-type mat+/mat– and *mat+ ΔPaNox3/mat– ΔPaNox3* heterocaryons were thus inoculated on media supplemented with a range of either $CaCl_2$ or EGTA concentrations. Fertility and growth rates of wild-type decreased as the concentration of calcium or EGTA increased up to concentrations for which the strain could not grow (0.75 mM EGTA and 1 M $CaCl_2$ on medium with dextrin, 0.50 mM EGTA and 500 mM $CaCl_2$ on medium with paper). The *ΔPaNox3* mutant displayed the same growth and fertility patterns as wild-type on all the media tested (data not shown).

To evaluate possible interactions between PaNox3 and the two other Nox, double and triple mutants strains of the three Nox genes were constructed (see *Experimental procedures* for construction of *PaNox1,3*, *PaNox2,3* and *PaNox1,2,3*). All the strains were investigated as the *ΔPaNox3* mutants. In all experiments, the double *PaNox1,3* and the triple *PaNox1,2,3* mutants behaved as the *IDC³⁴³* and *PaNox1,2* mutants, respectively, and the *PaNox2,3* double mutant behaved as the *ΔPaNox2* single mutant. Especially, NBT and DAB assays performed on the double and triple Nox mutants showed that in the double *PaNox1,3* and the triple *PaNox1,2,3* mutants NBT and DAB staining occurred with greater efficiency than in wild-type, with the same patterns as those observed in the *IDC³⁴³* and double *PaNox1,2* mutants respectively (Fig. S4). We thus concluded that *PaNox3* inactivation had no detectable effect in any of the conditions tested in the

laboratory, even when combined with other *Nox* mutations or when the Ca^{2+} concentration was modified.

PaNox1 *and* PaNox2 *regulate cellulose degradation*

We previously reported that *ΔPaNox2* has impaired capacity to exploit cellulosic substrates since it shows a diminished fertility with paper as the sole carbon source and inability to breach cellophane (Malagnac *et al.*, 2008). Inversely, We reported that fertility of the *IDC³⁴³* mutants affected in *PaNox1* could be restored when they were cultivated on a cellophane layer and transferred several times to a fresh medium (Malagnac *et al.*, 2004). Interestingly, solely replacing dextrin by a small piece of paper or several layers of cellophane as sole carbon source achieved a similar restoration of the *PaNox1* mutant fertility. This suggested that the carbon source (i.e. cellulose), rather than nitrogen or another nutrient was responsible for this fertility rescue. However, in the same conditions, fertility of the *PaNox1,2* double mutants (Malagnac *et al.*, 2004), as well as of the *ΔPaNoxR* mutants (Fig. 2) was not restored, suggesting antagonistic roles of PaNox1 and PaNox2 towards cellulose utilization. We thus further explored the ability of the mutants affected in *PaNox1*, *PaNox2*, *PaNox3* and *PaNoxR* to degrade cellulose, as this appears to be a key factor for completion of the sexual cycle in *P. anserina* grown on paper. We first directly evaluated the ability of the *Nox* mutants to breach cellophane layers, in comparison with wild-type (Table 1). In parallel, we estimated their cellulolytic capacities by measuring the loss of dry weight of filter papers, when used as sole carbon sources (Table 1). *ΔPaPls1*, the mutant inactivated in the *PaPls1* tetraspanin gene presenting the same phenotype as *ΔPaNox2* (Lambou *et al.*, 2008; Malagnac *et al.*, 2008) was also included in these analyses.

As seen in Table 1, the two methods apparently led to different results. Wild-type led to 36% loss of dry weight of filters in 7 days and breached one layer of cellophane after 3 days and then another one every 2 days. The

Table 1. Efficiency of the *P. anserina* Nox mutants to degrade cellulose.

	WT	Nox1	Nox2	Nox1,2	NoxR	Pls1	Nox3	Nox1,3	Nox2,3	Nox1,2,3
Cellophane breach in the absence of glucose (days)										
1 layer	3	4	>7	5	5	>7	3	4	>7	5
2 layers	5	7	>7	7	7	>7	5	7	>7	7
3 layers	7	>7	>7	>7	>7	>7	7	>7	>7	>7
Cellophane breach in the presence of glucose (days)										
1 layer	3	>7	>7	>7	>7	>7				
Net weight loss (%)										
3 days	7 ± 2	6 ± 2	2 ± 2	5 ± 2	5 ± 2	2 ± 2	7 ± 2	5 ± 4	2 ± 3	4 ± 2
5 days	25 ± 2	38 ± 2	13 ± 2	29 ± 3	24 ± 2	17 ± 2	28 ± 2	36 ± 3	15 ± 3	27 ± 3
7 days	36 ± 3	61 ± 4	27 ± 2	48 ± 4	43 ± 4	29 ± 3	39 ± 4	63 ± 4	29 ± 4	47 ± 3

'Cellophane breach' gives the number of days required to breach through the indicated numbers of cellophane layers.
'Net weight loss' gives in percentage the dry weight loss of 38 ± 0.7 mg circular filter pads 2.4 cm in diameter.

PaNox1 mutant degraded cellulose almost two times more efficiently, as it entailed a 61% weight loss in the same length of time. Yet, it breached the first layer after 4 days and then another one in 3 days. Remarkably, although the *ΔPaNox2* and *ΔPaPls1* mutants were slightly less efficient than wild-type in consuming cellulose (27% and 29% net dry weight loss at day 7 respectively), they could not breach a single layer of cellophane even after 7 days of incubation. At first glance, PaNox1 and PaNox2 appear to play opposite roles on cellulose degradation, with PaNox1 acting negatively and PaNox2 acting positively. Accordingly, the *PaNox1,2* double mutant and the *ΔPaNoxR* mutant showed intermediate phenotypes between those of *PaNox1* and *PaNox2* in both assays, thereby indicating that phenotypes of single mutants are compensated in the *PaNox1,2* and *ΔPaNoxR* mutants. In sharp contrast, inactivating *PaNox3* had no effect in any of the strains tested, confirming that PaNox3 plays a minor role in *P. anserina* (Table 1).

To understand at which level the cellulolytic activity is activated in the *IDC*[343] mutants affected in *PaNox1*, we have analysed global transcription profiles of these mutants in comparison to wild-type when they are grown for 24 h on cellophane. Data reported in Table 2 and Table S2 show that many putative cellulolytic genes are transcriptionally upregulated in *IDC*[343] mutants, while in general more genes are downregulated in these mutants

(657 versus 420 that are upregulated; Table 2). In addition to cellulases (glycoside hydrolases of the GH3, 5, 6, 12, 45, 61 and 94 families), the transcription factor *PaXyr1* encoded by Pa_1_23020 is two times more expressed in *PaNox1* mutants than in wild-type. The orthologues of this gene are known in *Hypocrea jecorina* and *Aspergillus niger* to regulate cellulases and xylanases, enzymes involved in hemicellulose/cellulose degradation (see Stricker *et al.*, 2008 for a review).

Nox functions are required for the development of cellular structures dedicated to the penetration of cellulose

The discrepancy between the cellulolytic activitiy and the capacity to breach cellophane layers observed in the mutants of *PaNox1* and *PaNox2* prompted us to investigate the modality of cellophane attack by *P. anserina* wild-type and Nox mutants at the cellular level. Microscopic observations were made on mycelium grown three to seven days on a layer of cellophane placed on solid medium in a Petri dish. The mycelium was mounted with the cellophane layer to directly observe the degradation process. Surprisingly, we observed that wild-type *P. anserina* was able to differentiate cellular structures permitting the development of the fungus within the cellophane (Fig. 4A and Supporting Material 'Wild Type

Table 2. Classification of genes differentially regulated in the *IDC*[343] strain versus wild-type as revealed by transcript profiling.

	Genes upregulated in *IDC*[343] fold change ≥ 2	Genes downregulated in *IDC*[343] fold change ≤ 2
Genes involved in cellulose degradation	26	1
Genes involved in lignin degradation	6	9
Other genes involved in carbohydrate degradation	55	19
Other genes with known function	111	239
Other genes with unknown function	222	389
Total	420	657

Regulated genes were defined as genes that displayed a |Fold Change| ≥ 2 and an adjusted *P*-value of ≤0.001.
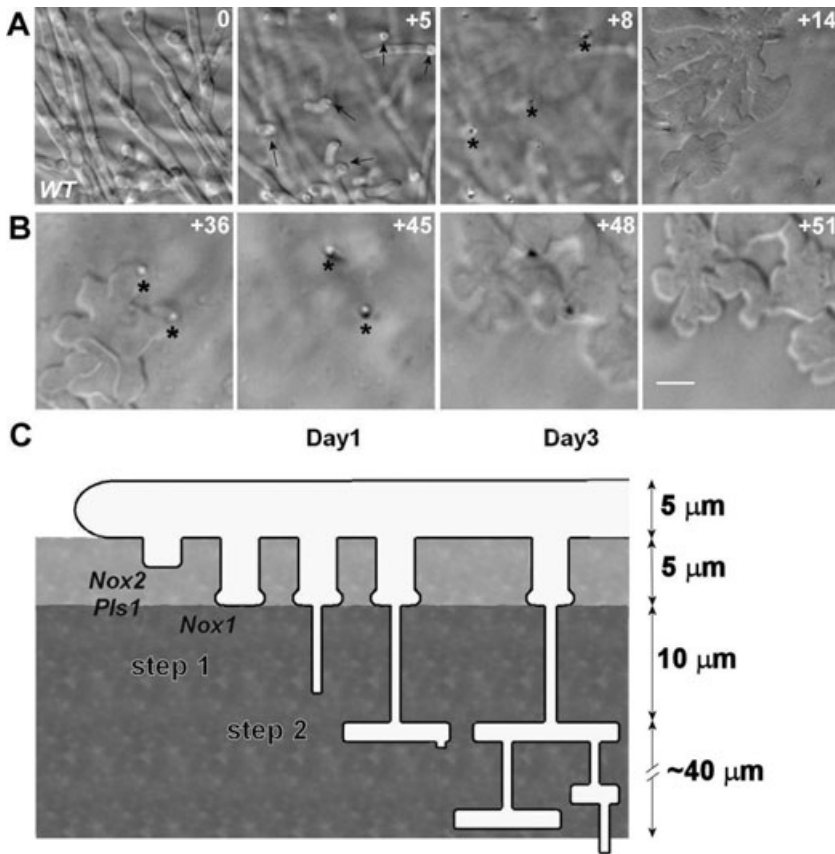
Fig. 4. Cellophane penetration by wild-type *P. anserina*.

A. Three-day-old wild-type mycelium growing on a cellophane layer. Numbers indicate the distance from the first picture in μm. Hyphae growing onto cellophane reorient their growth towards the cellophane and establish contacts that slightly bulge (+5; arrows). Then, needle-like hyphae emerge from these bulges and penetrate into the cellophane (+8). Within the cellophane, needle-like hyphae ('*' indicates some of them) give rise to mycelium that differentiates horizontally forming palm-like structures (+14).

B. Seven-day-old wild-type mycelium was removed from the cellophane prior mounting. Numbers indicate distance in μm from the surface onto which the mycelium had grown. Within the cellophane, the palm-like mycelium (+36) differentiates two needle-like hyphae (*) that grow further and give rise to a new palm-like mycelium deeper within the cellophane (+51). This is repeated until the fungus crosses the entire layer.

C. Schematic diagram representing the different steps during cellophane breach by wild-type *P. anserina*. In light grey is the area between horizontally growing hyphae and the bulged contacts that differentiate the needle-like hyphae. In dark grey is the cellophane layer breached by wild-type *P. anserina*. PaNox2 and PaPls1 functions are required for wild-type hyphal reorientation towards cellophane (step 1). PaNox1 function is required for the differentiation of needle-like hyphae (step 2). Bar scale: 10 μm.

1.tif'). Hyphae grew at first horizontally on the cellophane, then they produced branches (step 1, Fig. 4) that reoriented their growth perpendicularly towards the cellophane for about 5 μm, establishing contacts that bulged. Very thin needle-like hyphae emerged from these bulges (step 2. Fig. 4) and penetrated into the cellophane. When about 10 μm deep within the cellophane, the needle-like hyphae differentiated palm-like structures, perpendicularly to the direction of growth. This process was completed in about one day. New needle-like hyphae then emerged perpendicularly to the palm-like structures, went deeper into the cellophane and branched again, until the layer was crossed (Fig. 4B; Supporting Material 'Wild Type 2.tif'). We estimate that the length of these secondary needle-like hyphae is variable and can span up to 20 μm and that the fungus crossed the distance of about 60 μm before reaching the other side of the cellophane layer in 2–3 days. The *PaNox3* mutant behaved as wild-type, in line with its lack of phenotype. On the contrary, *IDC*[343], *ΔPaNox2*, *ΔPaNoxR*, *PaNox1,2* and *ΔPaPls1* were blocked before cellophane penetration. However, the mutants displayed different defects (Fig. 5).

The *IDC*[343] mutants of *PaNox1* were blocked at step 2, since hyphae of the mutants were able to reorient their growth towards the cellophane layer and establish promi-

nent bulges at the surface (Fig. 5 and Supporting Material 'Nox1.tif'). However, these bulges were defective in differentiating the needle-like hyphae that penetrated the cellophane. This resulted in accumulation of bulges in contact with cellophane, which was specific of the *PaNox1* mutants and was not seen in the other *Nox* mutants. As *IDC*[343], the *ΔPaNox2* mutants could not penetrate cellophane. However, they were impaired at step 1, since the reoriented hyphae did not grow towards the cellophane as wild-type and *IDC*[343] (Fig. 5 and Supporting Material 'Nox2.tif'). Interestingly, the *ΔPaPls1* and *ΔPaNoxR* mutants as well as the *PaNox1,2* double mutant displayed similar phenotypes as that of the *ΔPaNox2* mutant (Fig. 5 and Supporting Materials 'Nox1,2.tif', 'NoxR.tif' and 'Pls1.tif'). This showed that the *PaNox2* mutation was epistatic to the *PaNox1* mutation for this process and that *PaPls1*, *PaNox2* and *PaNoxR* were required before *PaNox1* for cellophane penetration (Fig. 4C).

The similarity of the regulation of the penetration process between *P. anserina* and some plant pathogens prompted us to test whether *P. anserina* could behave as a true plant pathogen. Breaching of onion skin is an assay classically performed to assess the ability of phytopathogens to penetrate into plant cells. We have thus assayed
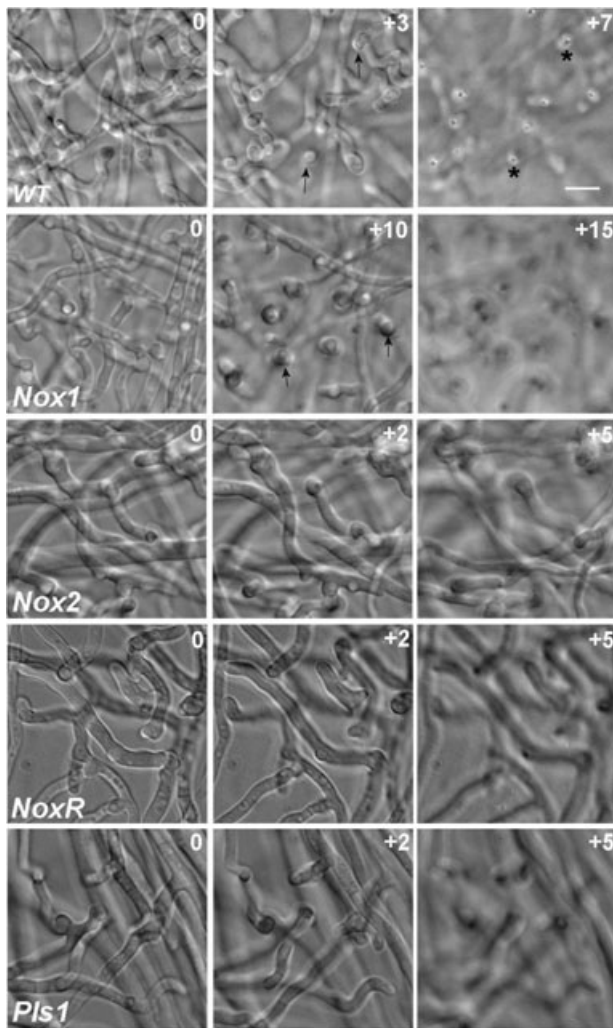
Fig. 5. Nox mutants are defective for cellophane penetration. Three-day-old mycelia of wild-type and mutant *P. anserina* strains grown on a cellophane layer were observed. Numbers indicate the distance from the first picture in μm. In the first column, mycelia of all the strains are growing horizontally on the cellophane layer. In the second column, mycelia of the wild-type and *IDC*[343] mutants (*Nox1*) reorient their growth towards the cellophane and establish bulging contacts (arrows). Strikingly, in the *IDC*[343] mutants, these contacts are more prominent but never differentiate needle-like hyphae, unlike wild-type. In the *ΔPaNox2* (*Nox2*), *ΔPaNoxR* (*NoxR*) and *ΔPaPls1* (*Pls1*) mutants, the hyphal reorientation towards cellophane is impaired and the contacts observed are less prominent. Note that the phenotype of *PaNox1,2* not shown here is identical to that of *ΔPaNoxR*. Also, the contacts made by these mutants can be deformed and a single hypha can repeatedly establish contacts that fail to penetrate the cellophane. In the third column, wild-type needle-like hyphae penetrate into the cellophane (*). In contrast, cellophane penetration is blocked in all the tested mutants. Bar scale: 10 μm.

whether wild-type and *Nox* mutants of *P. anserina* were able to penetrate onion epidermis as described (Gourgues *et al.*, 2004). On this substrate, all the strains grew poorly and none of them could cross the epidermis, nor did we observe structures resembling those involved in cellophane penetration.

Cellophane breaching and inhibition by glucose

Neither the mutants of *PaNox1* nor *PaNox2* penetrated cellophane, however, the *PaNox1* mutants were able to breach one layer of cellophane at a rate only slightly diminished when compared with wild-type, while the *PaNox2* mutants never breached a single layer. To check how the *Nox* mutants altered cellophane, we removed the mycelium and mounted the cellophane layer alone. For wild-type and the *ΔPaNox3* mutants, the cellophane was completely invaded by the fungus (Supporting Material 'Wild Type 2.tif'). As the fungus crossed the cellophane layer, the palm-like structures expanded horizontally. Accordingly, the mycelium grown onto the cellophane could hardly been separated from the cellophane itself. Furthermore, only small strips of cellophane could be retrieved from the medium before mounting, suggesting that the cellophane below the mycelium was largely degraded. In contrast, we never observed any hyphae developing inside cellophane for *IDC*[343], *ΔPaNox2*, *PaNox1,2*, *ΔPaNoxR* and *ΔPaPls1* mutants, even after 7 days of growth. The cellophane below the *ΔPaNox2* and *ΔPaPls1* mycelia remained nearly intact, easily separated from the mycelia and easily retrieved from the Petri dish, as already observed in cellophane breaching experiments. In sharp contrast, the cellophane below the *IDC*[343], *PaNox1,2* and *ΔPaNoxR* mycelia appeared greatly degraded, detaching from the medium as small stripes as in wild-type, an observation that agrees with their capacity to breach cellophane layers.

Cellulose degradation is a complex phenomenon culminating in the production of glucose that is then internalized into cells and metabolized. Hence, sensing the glucose gradient generated at hyphal tips when mycelium grows on cellophane might trigger reorientation of hyphal growth towards cellophane. In order to test the effect of glucose on this tropism, we have compared breaching and penetration of cellophane with or without glucose in the medium. We observed that adding glucose to the medium impairs cellophane breaching in wild-type and in the *IDC*[343] and *ΔPaNoxR* mutants. First, cellophane below mycelia of all the strains tested always appeared less degraded in presence of glucose. Second, the crossing of cellophane was delayed in the *IDC*[343] and the *ΔPaNoxR* mutants (Table 1), but not in wild-type.

We have then observed the penetration process of the different strains at the cellular level in the presence of glucose in the medium. In accordance with the cellophane breaching experiments, glucose did not block cellophane penetration in wild-type but did modify the penetration process. First, we observed that the needle-like hyphae were emitted from horizontally growing hyphae without prior reorientation (Fig. 6), suggesting that hyphal reorientation (step 1, Fig. 4C) was skipped in wild-type
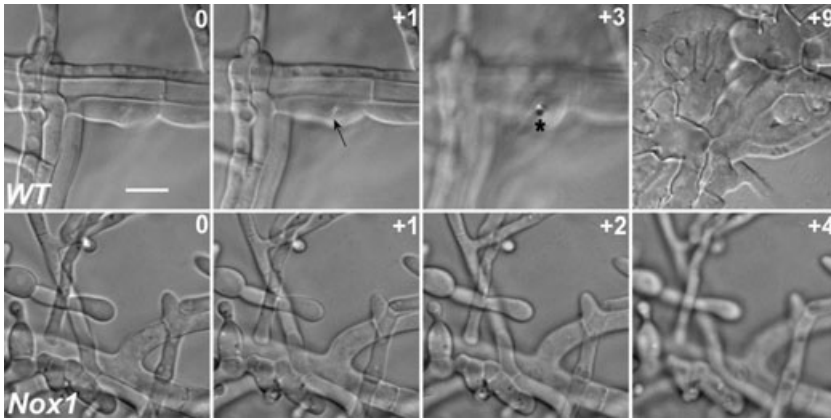
Fig. 6. Inhibitory effects of glucose on hyphal reorientation. Three-day-old mycelia of wild-type and *IDC³⁴³PaNox1* mutants growing on a cellophane layer overlaid on M3 medium containing glucose. The numbers indicate distance from the first picture in μm. In wild-type, the reorientation phase is skipped, since needle-like hyphae (*) are directly emitted from horizontally growing hyphae (arrow in +1). Note that the morphology of the palm-like structures (visible in +9) is modified in the presence of glucose. In the *IDC³⁴³* mutants (*Nox1*), hyphal reorientation is absent. Instead, hyphae tend to swell, to accumulate septa and to bud.
Bar scale: 10 μm.

P. anserina in the presence of glucose. The length of these needle-like hyphae was not modified (10 μm) when compared with those on medium-lacking glucose. We also observed that the morphology of palm-like structures was slightly different, possibly accounting for the observed diminished cellophane degradation. The reorientation step was also abolished in the *PaNox1* mutants. Indeed, as shown in Fig. 6, we never observed reorientation of hyphae nor accumulation of bulging contacts in the *IDC³⁴³* mutants in the presence of glucose. Instead, the mycelium tended to swell, to accumulate septa and to bud. Note that the *ΔPaNoxR* and *ΔPaNox2* mutants, which were defective for hyphal reorientation, showed similar modification of hyphal morphology on glucose, though less pronounced in the *ΔPaNox2* mutants (data not shown). Altogether, these data indicated that glucose inhibited hyphal reorientation and confirmed that hyphal reorientation (step 1) and emission of needle-like hyphae (step 2) were differently controlled.

Discussion

In a mutant screen designed to uncover genes involved in CG, we have identified *IDC⁵²⁴*, a mutant of the *P. anserina* p67^phox homologue, *PaNoxR*. This mutant contains a null allele of *PaNoxR* since it displays the same phenotype as the complete deletion of the coding sequence. Activation of Nox by p67^phox/NoxR and Rac is conserved in plants, in mammals and in the symbiotic fungus *E. festucae* (Takemoto *et al.*, 2006). In *IDC⁵²⁴*, the mutation that abolishes the PaNoxR function is a missense replacing a leucine by a proline in the putative Rac binding domain. This leucine is conserved among the Pezizomycotina and a change to a proline could greatly modify the structure of PaNoxR in this region. We propose that Rac could also regulate Nox function in *P. anserina* and that the effect of the mutation in *IDC⁵²⁴* is to abolish binding of Rac to PaNoxR.

We show that PaNoxR inactivation strictly recapitulates all the phenotypes of the *PaNox1,2* double mutants.

Therefore, PaNoxR activates both *PaNox1* and *PaNox2* in *P. anserina*, as described in *B. cinerea* and *N. crassa* (Cano-Dominguez *et al.*, 2008; Segmuller *et al.*, 2008). It is worth noting that the *PaNoxR* mutant does not display any supplementary phenotype as compared with the *PaNox1,2* double mutant. This suggests that in *P. anserina*, PaNoxR is probably only required for the activation of PaNox1 and PaNox2. However, we cannot rule out an effect on PaNox3, since we could not find a phenotype to test this possibility. Reciprocally, the *PaNox1* and *PaNox2* single and double mutants do not present any additional phenotypes when compared with the *PaNoxR* mutants. This led to the conclusion that activation of both PaNox1 and PaNox2 occurs essentially through PaNoxR and that PaNoxR is not responsible for the specificity of *PaNox1* and *PaNox2* in sexual reproduction and ascospore germination respectively. We propose that additional factors are involved in this specificity. The PaPls1 tetraspanin is a good candidate to confer specificity to PaNox2, since its inactivation displays the same phenotype as inactivation of PaNox2 (Lambou *et al.*, 2008; Malagnac *et al.*, 2008), while IDC1 could confer specificity to PaNox1 (Jamet-Vierny *et al.*, 2007). The genetic screen designed to uncover genes involved in CG (Haedens *et al.*, 2005) will likely yield new additional and promising candidates conferring specificity to PaNox1. Similarly, a genetic screen aimed at obtaining mutants affected in their germination potencies may permit to retrieve candidate genes involved in the specificity of PaNox2.

The discovery of a third Nox-encoding gene in the genome of *P. anserina*, *PaNox3*, prompted us to functionally test this gene. Our data show that PaNox3 does not perform any function during mycelium, fruiting body and ascospore development in laboratory conditions. From an evolutionary perspective, this suggests that Nox3 may not be as essential as Nox1 and Nox2 and that Nox3 could be required in very specific growth conditions that we have not been able to reproduce. This lack of obvious role in

P. anserina physiology is in agreement with our phylogenetic analysis, indicating that fungal *Nox3* genes are under less intense selective pressure than the Nox1 and Nox2 genes and that this third isoform has been lost repeatedly in the course of fungal evolution.

Our data clearly demonstrate that PaNox3 is not a source of ROS detected by the DAB and NBT staining assays. Yet, we have not determined what could account for increased DAB and NBT staining in the different *P. anserina Nox* mutants, i.e. *IDC*[343], *PaNox1,2* and *ΔPaNoxR*. Interestingly, in *A. nidulans*, disruption of *NoxA* also leads to increased NBT staining on the whole mycelium (Semighini and Harris, 2008) and the *ΔNox1 ΔNox2* double mutant of *M. grisea* displays enhanced NBT staining at hyphal tips (Egan *et al.*, 2007). DAB and NBT are supposed to precipitate once reduced in the presence of peroxide and superoxide respectively. While DAB reduction requires a peroxidase activity, NBT reduction by superoxide is not enzymatic. The possibility exists that redox enzymes produced by *P. anserina* perform reductions of either DAB or NBT. Indeed, searches of the *P. anserina* complete genome sequence reveal a plethora of genes encoding such enzymes. First, there are additional more divergent *Nox* homologues. These are more closely related to ferric reductases that reduce metal ions before they can be imported into the cell (Kosman, 2003; Bedard *et al.*, 2007). Ten such CDS presenting a significant resemblance to ferric reductases (score $< 10^{-5}$ in BLAST queries, P. Silar, unpubl. data) are present in the *P. anserina* genome. They are highly divergent from each other and some are quite divergent from the known ferric reductases. It cannot be excluded that, instead of reducing metal, these proteins generate peroxide or superoxide or may even enzymatically reduce small molecules such as DAB and NBT. Their actual roles therefore remain to be determined. Second, potential sources of superoxide are present in *P. anserina* since the genome contains two CDS with similarity to lipoxygenase (Pa_2_4370 and Pa_6_8140) and two CDS with similarity to prostaglandin H synthase (Pa_5_1240 and Pa_1_4690). In mammalian and plant cells, these redox enzymes are known to harbour a DPI-insensitive Nox activity and to generate superoxide anions (Kukreja *et al.*, 1986; Roy *et al.*, 1994; O'Donnell and Azzi, 1996). Third, a previous BLAST analysis (Espagne *et al.*, 2008) detected many genes potentially participating in lignocellulose degradation through peroxide production. This enzymatic set includes 29 CDS similar to Glucose/Methanol/Choline (GMC) oxidoreductases (Cavener, 1992; Leskovac *et al.*, 2005), many of which are likely to be secreted, two cellobiose dehydrogenases (Bao *et al.*, 1993), one pyranose oxidase (Leitner *et al.*, 2001), one galactose oxidase (van der Meer *et al.*, 1989) and one copper radical oxidase (Kersten and Cullen, 1993). Homologues of these genes are known or suspected in basidiomycota to produce peroxide or perform redox modifications of small substrates during lignocellulose degradation (ten Have and Teunissen, 2001; Wesenberg *et al.*, 2003; Martinez *et al.*, 2005). This list is evidently not exhaustive and numerous other enzymes could be involved.

This third set of enzyme involved in plant biomass degradation is of particular interest since one interesting point that emerges from the present study is the connection between *Nox* genes and cellulose degradation in *P. anserina* (Malagnac *et al.*, 2008). Our microarray analysis indicates that glycoside hydrolases are transcriptionnaly upregulated in the mutants of *PaNox1*, in line with an upregulation of PaXyr1, a transcription factor whose orthologues in *A. niger* and *H. jecorina* are known to regulate carbohydrate degradation genes (Stricker *et al.*, 2008). Glycoside hydrolase do not act alone and many additionnal enzymes are known to participate in cellulose/plant biomass degradation (Wesenberg *et al.*, 2003). It is noteworthy that this enzymatic set is known to produce ROS. Given the correlation between increased DAB/NBT staining and increased cellulose degradation in the mutants of *PaNox1*, we speculate that the DAB and NBT assays may betray the activity of this enzymatic machinery. One of the multiple roles of Nox signalling would thus be to regulate the production of these enzymes in response to the nature and availability of the carbon source. PaNox1 would repress their production, while PaNox2 would activate it or be involved in a more subtle regulation, such as their correct localization (see below). In addition to quantitative defects in cellulose degradation, the mutants of *PaNox1* and *PaNox2* exhibit developmental defects, which impair their capacity to degrade cellophane. We show here that the saprobe *P. anserina* differentiates specialized cells able to penetrate and develop within a solid substrate in two steps. Indeed, hyphae growing onto cellophane first reorient themselves perpendicularly towards the substrate and establish bulged contacts. Then, from these bulges differentiate needle-like hyphae that allow the fungus to penetrate into cellophane, to develop within it and finally to cross it. This process strikingly resembles the appressorium-mediated penetration performed by numerous phytopathogenic fungi to breach into their host. Moreover, both PaNox1 and PaNox2 are required for the normal development of the structures dedicated to the penetration of cellophane. The mutants of *PaNox1* correctly reorient hyphae towards cellophane and efficiently make the bulged contacts with the surface. However, these bulges are blocked and never differentiate needle-like hyphae. The mutants of *PaNox2* are affected at an earlier stage than the mutants of *PaNox1*. Indeed the
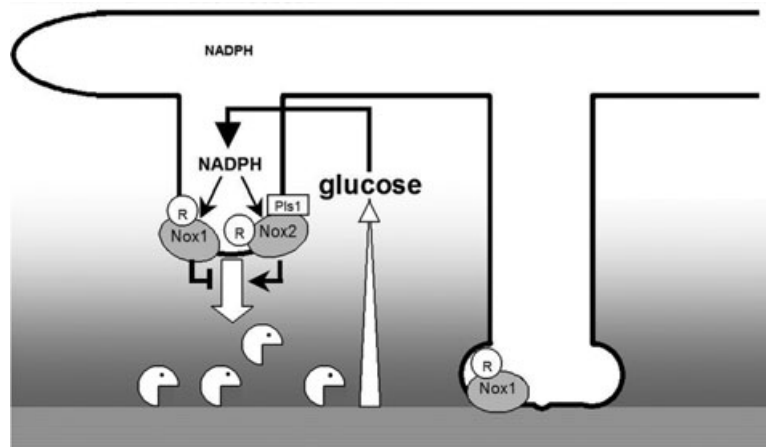
Fig. 7. Nutrient sensing and cellophane penetration. Fungi are well known to secrete enzymes at hyphal tips to degrade their growth substrate for nutrient supply. We propose that the proper targeting of the enzymatic battery devoted to cellulose degradation is controlled by PaNox2 and PaPls1 in *P. anserina*. In wild-type, cellophane is degraded into glucose monomers at hyphal tips, generating a glucose gradient. Once imported into the cell, the glucose is catabolized and the intracellular level of NADPH increases. This in turn leads to activation of Nox enzymes specifically at hyphal tips. This positive regulatory loop triggers reorientation of hyphae towards glucose gradient and hence, towards cellophane. On the contrary, PaNox1 would act as a brake to slow down the system and to avoid wasteful consumption of nutrients and enzymes. Moreover, PaNox1 function would also be required later for differentiation of the needle-like hyphae that allow penetration of the cellophane. R = PaNoxR.

ΔPaNox2 mutants are affected in the reorientation process and establishment of the bulges that contact the surface of the substrate. Default of penetration is shared by *Nox1* and *Nox2* mutants in *M. grisea* and *Nox2* mutant in *B. cinerea* (Egan *et al.*, 2007; Segmuller *et al.*, 2008). It will be of great interest to address the question of whether the structures described here in the saprobe *P. anserina* are truly akin to appressoria. Especially, in the view that *P. anserina* does not behave as a phytopathogen, since it is unable to penetrate living material, as the onion skin assay indicates. In nature, *P. anserina* has only been observed on herbivore dung.

The combination of both quantitative and qualitative effects on cellulose degradation nicely explains the phenotypes of the *PaNox1* and *PaNox2* single and double mutants. Indeed, even though they cannot penetrate cellophane, the *PaNox1* mutants would be able to breach cellophane because they possess enhanced cellulolytic capacity and correctly target the degradation machinery towards the substrate. They establish huge numbers of contacts with the substrate compared with wild-type and the *PaNox2* mutants, allowing them to efficiently degrade cellulose without penetration. This high activity would ensure sufficient nutrient scavenging, accounting for the observed rescue of fertility on paper and cellophane. In contrast to the *PaNox1* mutants, the *PaNox2* mutants, which are defective in establishing efficient and/or polarized contacts with the cellophane surface, would not target properly their degradation machinery. As a consequence, the *PaNox2* mutants would be incapable of breaching cellophane. This could also account for their slightly dimin-

ished capacity to degrade filter paper. This impaired capacity of the *PaNox2* mutants to utilize cellulose as carbon source should negatively impact on their sexual reproduction, as observed. Remarkably, the mutants of *PaPls1* harbour the very same defaults as the mutants of *PaNox2*, thus emphasizing a common role of *PaPls1* and *PaNox2* in regulating cellulose degradation. We propose that in the *PaNox1,2* and *ΔPaNoxR* mutants, enhancement of the degradation capacity (promoted by lack of PaNox1) is counterbalanced by impaired targeting of the degradation machinery (promoted by lack of PaNox2). Accordingly, the *PaNox1,2* and *ΔPaNoxR* mutants show a lower cellulolytic activity than the *PaNox1* mutant, as measured by loss of dry weight of filter paper, but are able to breach cellophane more slowly than the mutants of *PaNox1*. In contrast to the mutants of *PaNox1*, they would remain female sterile on paper and cellophane, because they would not scavenge enough nutrients.

It is as yet too early to know whether the ROS generated by the Nox enzymes are used solely for signalling purposes or whether they also directly participate in the degradation process. Whatever the roles of Nox enzymes, a simple feedback regulatory loop in the signalling cascade could explain many of the results presented here, including the surprising increased degradation of cellulose by the mutants of *PaNox1* (Fig. 7). Indeed, cellulose degradation results in the generation of glucose with a gradient of high concentration near the cellulose fibres. Further developmental processes exploiting this gradient would ensure optimal carbon retrieval. In areas with high levels of glucose, the hyphae should contain

high levels of intracellular NADPH and hence display high levels of PaNox1 and PaNox2 activity. This would as a first step promote a reorientation of growth towards the glucose source under the control of PaNox2 and then decrease the production/secretion of enzymes through PaNox1. In this process, PaNox2 together with PaPls1 would be required to target growth and the degradation machinery towards high glucose concentrations. On the contrary, PaNox1 would act as a regulator to slow down degradation in order to avoid wasteful consumption of enzymes and substrate. It would also control in a second step the differentiation of the needle-like hyphae. Note that PaNoxR and probably other factors, such as Rac, could participate in the fine tuning of PaNox1 versus PaNox2 activities. PaNox1 could for instance downregulate PaNox2 by starving PaNox2 for these factors. PaNox1 and PaNox2 could also possibly compete for NADPH. In our model, glucose represents a key factor controlling tropism towards cellophane. In agreement, our data indicate that tropism towards cellophane is inhibited when the glucose gradient is altered. Interestingly, in the presence of glucose, wild-type *P. anserina* is still able to differentiate needle-like hyphae and palm-like cells that allow the fungus to grow within cellophane, suggesting that the control of these structures is independent from glucose availability.

Similar roles of Nox in the degradation of complex carbon sources in other fungal systems could account for the somewhat contrasting phenotypes observed in the various fungal *Nox* mutants. For example, uncontrolled production of enzymes degrading plant cell walls by the *NoxA* and *NoxR* mutants of the mutualistic fungus *E. festucae* could explain why these mutants display anarchic and invasive growth *in planta*, leading to loss of symbiosis and premature senescence of the host (Takemoto *et al.*, 2006; Tanaka *et al.*, 2006). Note that this fungus lives between the plant cells and should not breach them. Reciprocally, impaired sensing of nutrients or penetration of plant cell wall could account for impaired *in planta* development of the Nox mutants in *M. grisea*, *B. cinerea* and *C. purpurea* (Egan *et al.*, 2007; Giesbert *et al.*, 2008; Segmuller *et al.*, 2008).

Finally, on a broader perspective, we previously showed that the germination process of *P. anserina* ascospores reassembles the appressorium-mediated plant penetration (Lambou *et al.*, 2008). Here, we report the generation by *P. anserina*, an exclusively saprobic fungus, of structures dedicated to breach plant materials. A tempting hypothesis is that the difference between saprobic, parasitic and mutualistic fungal lifestyles may not be so great, and at least may not involve in saprobes the inability to breach the plant cell wall. This could account in part for the recurrent changes of trophic lifestyles exhibited by eumycetes.

Experimental procedures

Strains and culture conditions

The strains were all derived from the S strain ensuring a homogenous genetic background (Rizet, 1952). The analysis of the single *IDC³⁴³* and *ΔPaNox2* mutants inactivated for *PaNox1* and *PaNox2*, respectively, as well as the double *IDC³⁴³ ΔPaNox2* mutants (here called *PaNox1,2*) have been described (Malagnac *et al.*, 2004). The *pks1–193* mutant harbouring a mutation in the polyketide synthase gene acting at the first step of melanin synthesis has been described previously (Picard, 1971; Coppin and Silar, 2007). This allele does not modify the pattern of DAB and NBT staining (Malagnac *et al.*, 2004), but by eliminating the pigment, it facilitates the assays. Standard culture conditions, media and genetic methods for *P. anserina* have been described (Rizet and Engelmann, 1949) and in http://podospora.igmors.u-psud.fr. The composition of the M0 and M3 media is the same as that of the M2 medium except that dextrin is replaced by glucose in the M3 medium while no carbon source is added in the M0 medium. Sterilized 3 MM Whatman paper (Cat. No. 3030917) was cut to the appropriate size (3 cm × 3 cm) and autoclaved only once before being overlaid onto M0 medium to be used as carbon source.

The methods used for nucleic acid extraction and manipulation have been described (Altschul *et al.*, 1990; Lecellier and Silar, 1994). Transformation of *P. anserina* protoplasts was carried out as described previously (Brygoo and Debuchy, 1985).

Complementation of IDC⁵²⁴ and deletion of PaNoxR

To complement the *IDC⁵²⁴* mutant, wild-type genomic DNA was amplified by PCR with primers Pa67fw_1 (AGAACC CCATTCGCACAA) and Pa67rev_1 (CCCTCGCCCTCCTAC TCT). Amplified DNA (15 µg) were used in co-transformation with 5 µg of pBC-phleo (Silar, 1995). Phleomycin-resistant transformants were then examined for thallus pigmentation and tested for fertility.

To delete *PaNoxR*, A 514-bp-long *PaNoxR* 5′ non-coding fragment was PCR-amplified using the forward primer Pa67–1 (AAGCTTCAGTAGGGCGGAGGAACA) located at positions −614 to −597 and the reverse primer Pa67–2 (ATC-GATTGAAACTTGGGCGGTTGT) located at positions −112 to −96. Positions are relative to the first base of the CDS. A 497 pb long PaNoxR 3′ non-coding fragment was PCR-amplified using the forward primer Pa67–3 (TCTAGAGC-GACGCGCAAAATCT) located at position 1968–1983 and the reverse primer Pa67–4 (AAGCTTCAAAACCCTCCTC-CTCCTCT) located at position 2433–2453. Both fragments were cloned into pGEMT vector (Promega). The PaNoxR 5′ and PaNoxR 3′ fragments were released from pGEMT by HindIII/ClaI and HindIII/XbaI double digestion respectively. Finally, both fragments were cloned in tandem into the pBC-hygro plasmid (Silar, 1995) at the XbaI/ClaI sites, generating the pBC-PaNoxR plasmid (see Fig. S5A and B for a schematic representation of the PaNoxR deletion strategy). Transformation of *P. anserina Δmus51::su8–1, pks1–193* strain (Lambou *et al.*, 2008) was performed using 10 µg of the pBC-PaNoxR plasmid previously linearized at the unique

HindIII site to generate homologous recombination ends. Six hygromycine B-resistant transformants (H^R) were obtained. All six transformants showed a similar phenotype as the *IDC^{524}* mutants (e.g. female sterility and impaired ascospore germination), suggesting disruption of *PaNoxR* by homologous recombination. Two transformants (Δ*PaNoxR_4* and Δ*PaNoxR_6*) were crossed with wild-type and *mus51$^+$pks1–193 H^R* spores, which germinated spontaneously on M2 medium plus hygromycine B were selected. Mycelia of these transformants were fragmented and monokaryotic mycelia of the *pks1–193 ΔPaNoxR::H^R* genotype were selected. These were crossed with wild-type on M2 medium supplemented with tricyclazol to avoid melanin deposition into the ascospore cell wall, thus allowing pks1$^+$, H^R spores to spontaneously germinate on M2 medium supplemented with hygromycine B (Coppin and Silar, 2007). Mycelia obtained from ascospores that germinated spontaneously were fragmented and monokaryotic *ΔPaNoxR::H^R* strains were selected. One strain of each mating type (+ and −) was selected for Δ*PaNoxR_4* and Δ*PaNoxR_6*. Confirmation of the deletion in both transformants was performed by Southern Blot analysis (Fig. S5C). Δ*PaNoxR_4* was selected for further studies. This mutant was co-transformed with pBC-phleo and a DNA fragment containing the *PaNoxR* wild-type gene, amplified from wild-type DNA with primers Pa67fw_1 and Pa67rev_1. Five phleomycin-resistant transformants among 24 regained a wild-type phenotype, confirming that the observed phenotypes were due to the deletion of P*aNoxR*.

Deletion of PaNox3

A 1891-bp-long *PaNox3* 5′ non-coding fragment was PCR-amplified using primers NOX3F1 (ATTCTAGACGATTTC-CATTGCTGTTCAA) located at positions −1926 to −1907 and NOX3R1 (ATGCGGCCGCATTGGCTCGAGGAAGAGGAT) located at positions −55 to −36. Positions are relative to the first base of the coding sequence. A 1769-pb-long *PaNox3* 3′ non-coding fragment was PCR-amplified using primers NOX3F2 (ATGGGCCCTACACCCACACGTGAATGG) located at positions 2331–2349 and NOX3R2 (ATTCTAGAAAGCGTTTAGCAGGTGAGGA) located at positions 4080–4099. Both fragments were cloned into the pGEMT vector (Promega). Because an XbaI site and a NotI site are present in NOX3F1 and NOX3R1, respectively, the corresponding 5′ non-coding fragment was released from the pGEMT vector by performing a XbaI/NotI double digest and cloned into the pBC-hygro plasmid at the XbaI/NotI sites. An ApaI site in NOX3F2 and an XbaI site in NOX3R2 allowed the released from the pGEMT vector of the corresponding 3′ non-coding fragment, which was then cloned in the XbaI/NotI sites into the plasmid harbouring the *PaNox3* 5′ non-coding fragment, generating pΔPaNox3 plasmid (see Fig. S6A and B for a schematic representation of the *PaNox3* deletion strategy). *P. anserina* transformation was performed using 10 μg of the pΔPaNox3 plasmid previously linearized at the unique XbaI site to generate homologous recombination ends. 58 H^R transformants were obtained and 13 of these were selected for further analysis. Their DNA was analysed by PCR with the Nox3F3 (TCTCAGCATGTCGCGGTA) and Nox3R3 (CTCTGATCGCGACGGTTT)

primers. This couple of oligonucleotides allows amplification of a fragment internal to the deleted cassette. DNA from three transformants did not permit to amplify the internal fragment, suggesting that *PaNox3* was removed from these transformants. Confirmation of the deletion in the three transformants was made by Southern Blot analysis (Fig. S6C). One transformant *ΔPaNox3* was selected for further phenotypic analyses. It was crossed with wild-type, and *ΔPaNox3 mat+* and *ΔPaNox3 mat–* strains were recovered in the progeny. The *ΔPaNox3* mutant was crossed with the *IDC^{343}* and *ΔPaNox2* mutants to construct both double mutants *PaNox1,3* and *PaNox2,3* respectively. The *PaNox1,2,3* triple mutant was then constructed by crossing the *PaNox1,3* double mutant with the *PaNox2,3* double mutant.

Phenotypic analysis

Fertility was evaluated as described (Rizet and Engelmann, 1949), except that the medium used was M2. Longevity was measured as in Silar and Picard (1994). CG was evaluated as in Silar *et al.* (1999), hyphal interference as in Silar (2005), and DAB and NBT staining as in Malagnac *et al.* (2004).

For breach experiments, cellophane was purchased from Bio-Rad (Cat. No. 165-0922). One, two or three layers of 7.5 cm disks of sterilized cellophane were overlaid onto 8 cm Petri plates filled with M2 or M3 medium. The cultures were inoculated at the centre of the plate and incubated for various lengths of time. Removing the disks and observing hyphae in the underlying medium determined breach of cellophane. The experiments were repeated independently at least three times.

To measure loss of dry weight, filters from Whatman (grade G540, Cat. No. 1540324) were autoclaved once and put onto an 8 cm Petri plate filled with M0 medium. The cultures were inoculated as the centre of the filter and after various times of incubation, the paper was removed and dried before weigh-in. We estimated the weight loss with the following calculation: (initial cellulose weight – remaining cellulose + mycelium weight)/initial cellulose weight. The data are an average (± SD) of nine measurements.

Microscopic analysis

Microscopic observations were made on mycelia growing on cellophane placed on solid medium in a Petri dish. M3 medium was used to assay glucose effects. Small pieces (1 cm^2) of cellophane with the mycelium were cut with a scalpel and mounted in water. To fully observe and characterize penetration of the cellophane by *P. anserina*, the piece of cellophane was mounted with mycelium either side up or up side down. To observe growth within the cellophane, we removed the mycelium from the cellophane layer prior to mounting up side down. Pictures were taken with a Leica microscope (Bannockburn, IL) DMIRE 2. Since penetration of the cellophane occurs perpendicularly to the surface, pictures were generated every micrometer to follow the process. Stacks of pictures were analysed with ImageJ (http://rsb.info.nih.gov/ij). Quantitative measurements of cellular structures were made on at least 11 samples.

RNA isolation and gene expression array-based hybridization

For RNA extraction, *mat* + wild-type and *IDC^343^* strains were grown for 24 h at 28°C on cellophane sheet overlaid on Petri dishes with M2 medium. Biological materials were collected and flash-frozen in liquid nitrogen. Total RNA of *P. anserina* was extracted using the RNeasy Plant Mini Kit (Qiagen), including a grinding process using a Mikro-dismembrator (Sartorius) and a DNase treatment. The quality and quantity of the total RNA was determined by using a Nanodrop spectrophotometer (Nanodrop Technologies) and the Bionalyzer 2100 system (Agilent Technologie).

The description of the microarray will be published elsewhere (Bidard *et al.*, Fungal Genetics Conference, Edinburgh, 2008 and manuscript in preparation). Target preparation, hybridization and washing were done following the two-colour microarray-based gene expression analysis instructions (version 5.0, February 2007) as described by the manufacturer (Agilent technologies). One-microgram aliquots of total RNA were labelled using the Low RNA input fluorescent linear amplification (LRILAK) PLUS kit (Agilent Technologies); internal standards came from the Two-color RNA spike kit (Agilent technologies). The labelling efficiencies and the product integrities were checked as described (Imbeaud and Auffray, 2005). A total of 825 ng of each of the Cy3- and Cy5-labelled targets were mixed and hybridized to the 4X44k *P. anserina* custom oligonucleotide microarrays (Agilent Technologies) representing the totality of the 10546 identified CDSs. Microarray slides were hybridized for 17 h at 65°C, in a rotating oven at 10 r.p.m. using the Agilent *in situ* hybridization kit. The slides were washed and then any traces of water were removed by centrifugation at 800 r.p.m. for 1 min.

Microarray experiment was done with a reference design with no dye swap. Experimental samples were labelled with Cy5 dye and reference samples with Cy3. The data are a representation of four biological replicates. The reference sample is made with a mixture of RNA extracted from different growth conditions (Bidard *et al.*, Fungal Genetics Conference, Asilomar, 2007 and manuscript in preparation).

For microarray data acquisition, processing and analysis, microarrays were scanned using the Agilent Array Scanner at 5 μm per pixel resolution with the eXtended Dynamic Range (XDR) function. Pre-processing treatment were performed with Feature Extraction (v9.5.3) software (Agilent technologies), with the GE2-v4–95_Feb07 default protocol and statistical differential analysis using the MAnGO software (Marisa *et al.*, 2007), moderate *t*-test with adjustment of *P*-values (Benjamini and Hochberg, 1995) was computed to measure the significance with each expression difference.

Acknowledgements

References

Aguirre, J., Rios-Momberg, M., Hewitt, D., and Hansberg, W. (2005) Reactive oxygen species and development in microbial eukaryotes. *Trends Microbiol* **13:** 111–118.

Altschul, S.F., Gish, W., Miller, W., Myers, E.W., and Lipman, D.J. (1990) Basic local alignment search tool. *J Mol Biol* **215:** 403–410.

Bao, W., Usha, S.N., and Renganathan, V. (1993) Purification and characterization of cellobiose dehydrogenase, a novel extracellular hemoflavoenzyme from the white-rot fungus *Phanerochaete chrysosporium*. *Arch Biochem Biophys* **300:** 705–713.

Bedard, K., Lardy, B., and Krause, K.H. (2007) NOX family NADPH oxidases: not just in mammals. *Biochimie* **89:** 1107–1112.

Benjamini, Y., and Hochberg, Y. (1995) Controlling the false discovery rate: a practical and powerful approach to multiple testing. *J R Stat Soc Ser B* **57:** 289–300.

Brygoo, Y., and Debuchy, R. (1985) Transformation by integration in *Podospora anserina*. I. Methodology and phenomenology. *Mol Gen Genet* **200:** 128–131.

Cano-Dominguez, N., Alvarez-Delfin, K., Hansberg, W., and Aguirre, J. (2008) NADPH oxidases NOX-1 and NOX-2 require the regulatory subunit NOR-1 to control cell differentiation and growth in *Neurospora crassa*. *Euk Cell* **7:** 1352–1361.

Cavener, D.R. (1992) GMC oxidoreductases. A newly defined family of homologous proteins with diverse catalytic activities. *J Mol Biol* **223:** 811–814.

Chen, J., Zheng, W., Zheng, S., Zhang, D., Sang, W., Chen, X. *et al.* (2008) Rac1 is required for pathogenicity and Chm1-dependent conidiogenesis in rice fungal pathogen *Magnaporthe grisea*. *PLoS Pathog* **4:** e1000202.

Coppin, E., and Silar, P. (2007) Identification of PaPKS1, a polyketide synthase involved in melanin formation and its utilization as a genetic tool in *Podospora anserina*. *Mycol Res* **111:** 901–908.

Egan, M.J., Wang, Z.Y., Jones, M.A., Smirnoff, N., and Talbot, N.J. (2007) Generation of reactive oxygen species by fungal NADPH oxidases is required for rice blast disease. *Proc Natl Acad Sci USA* **104:** 11772–11777.

El-Khoury, R., Sellem, C.H., Coppin, E., Boivin, A., Maas, M.F., Debuchy, R., and Sainsard-Chanet, A. (2008) Gene deletion and allelic replacement in the filamentous fungus *Podospora anserina*. *Curr Genet* **53:** 249–258.

Espagne, E., Lespinet, O., Malagnac, F., Da Silva, C., Jaillon, O., Porcel, B.M. *et al.* (2008) The genome sequence of the model ascomycete fungus *Podospora anserina*. *Genome Biol* **9:** R77.

Giesbert, S., Schurg, T., Scheele, S., and Tudzynski, P. (2008) The NADPH oxidase Cpnox1 is required for full pathogenicity of the ergot fungus *Claviceps purpurea*. *Mol Plant Pathol* **9:** 317–327.

Gourgues, M., Brunet-Simon, A., Lebrun, M.H., and Levis, C. (2004) The tetraspanin BcPls1 is required for appressorium-mediated penetration of Botrytis cinerea into host plant leaves. *Mol Microbiol* **51:** 619–629.

Haedens, V., Malagnac, F., and Silar, P. (2005) Genetic control of an epigenetic cell degeneration syndrome in *Podospora anserina*. *Fung Genet Biol* **42:** 564–577.

ten Have, R., and Teunissen, P.J. (2001) Oxidative mechanisms involved in lignin degradation by white-rot fungi. *Chem Rev* **101:** 3397–3413.

Hibbett, D.S., Binder, M., Bischoff, J.F., Blackwell, M., Cannon, P.F., Eriksson, O.E. *et al.* (2007) A higher-level phylogenetic classification of the Fungi. *Mycol Res* **111:** 509–547.

Imbeaud, S., and Auffray, C. (2005) 'The 39 steps' in gene expression profiling: critical issues and proposed best practices for microarray experiments. *Drug Discov Today* **10:** 1175–1182.

Jamet-Vierny, C., Debuchy, R., Prigent, M., and Silar, P. (2007) *IDC1*, a Pezizomycotina-specific gene that belongs to the PaMpk1 MAP kinase transduction cascade of the filamentous fungus *Podospora anserina. Fung Genet Biol* **44:** 1219–1230.

Katoh, K., Kuma, K.-i., Toh, H., and Miyata, T. (2005) *MAFFT* Version 5: improvement in accuracy of multiple sequence alignment. *Nucl Acids Res* **33:** 511–518.

Kersten, P.J., and Cullen, D. (1993) Cloning and characterization of cDNA encoding glyoxal oxidase, a H2O2-producing enzyme from the lignin-degrading basidiomycete *Phanerochaete chrysosporium. Proc Natl Acad Sci USA* **90:** 7411–7413.

Kicka, S., and Silar, P. (2004) PaASK1, a mitogen-activated protein kinase kinase kinase that controls cell degeneration and cell differentiation in *Podospora anserina. Genetics* **166:** 1241–1252.

Kicka, S., Bonnet, C., Sobering, A.K., Ganesan, L.P., and Silar, P. (2006) A mitotically inheritable unit containing a MAP kinase module. *Proc Natl Acad Sci USA* **103:** 13445–13450.

Kosman, D.J. (2003) Molecular mechanisms of iron uptake in fungi. *Mol Microbiol* **47:** 1185–1197.

Kukreja, R.C., Kontos, H.A., Hess, M.L., and Ellis, E.F. (1986) PGH synthase and lipoxygenase generate superoxide in the presence of NADH or NADPH. *Circ Res* **59:** 612–619.

Lalucque, H., and Silar, P. (2003) NADPH oxidase: an enzyme for multicellularity? *Trends Microbiol* **11:** 9–12.

Lambou, K., Malagnac, F., Barbisan, C., Tharreau, D., Lebrun, M.H., and Silar, P. (2008) A crucial role for the Pls1 tetraspanin during ascospore germination of the saprophytic fungus *Podospora anserina. Euk Cell* **7:** 1809–1818.

Lara-Ortiz, T., Riveros-Rosas, H., and Aguirre, J. (2003) Reactive oxygen species generated by microbial NADPH oxidase NoxA regulate sexual development in *Aspergillus nidulans. Mol Microbiol* **50:** 1241–1255.

Lecellier, G., and Silar, P. (1994) Rapid methods for nucleic acids extraction from Petri dish grown mycelia. *Curr Genet* **25:** 122–123.

Leitner, C., Volc, J., and Haltrich, D. (2001) Purification and characterization of pyranose oxidase from the white rot fungus *Trametes multicolor. Appl Environ Microbiol* **67:** 3636–3644.

Leskovac, V., Trivic, S., Wohlfahrt, G., Kandrac, J., and Pericin, D. (2005) Glucose oxidase from Aspergillus niger: the mechanism of action with molecular oxygen, quinones, and one-electron acceptors. *Int J Biochem Cell Biol* **37:** 731–750.

Malagnac, F., Bidard, F., Lalucque, H., Brun, S., Lambou, K., Lebrun, M.H., and Silar, P. (2008) Convergent evolution of morphogenetic processes in fungi: Role of tetraspanins and NADPH oxidases 2 in plant pathogens and saprobes. *Comm Int Biol* **1:** 180–181.

Malagnac, F., Lalucque, H., Lepere, G., and Silar, P. (2004) Two NADPH oxidase isoforms are required for sexual reproduction and ascospore germination in the filamentous fungus *Podospora anserina. Fung Genet Biol* **41:** 982–997.

Marisa, L., Ichante, J.L., Reymond, N., Aggerbeck, L., Delacroix, H., and Mucchielli-Giorgi, M.H. (2007) MAnGO: an interactive R-based tool for two-colour microarray analysis. *Bioinformatics* **23:** 2339–2341.

Martinez, A.T., Speranza, M., Ruiz-Duenas, F.J., Ferreira, P., Camarero, S., Guillen, F. *et al.* (2005) Biodegradation of lignocellulosics: microbial, chemical, and enzymatic aspects of the fungal attack of lignin. *Int Microbiol* **8:** 195–204.

van der Meer, R.A., Jongejan, J.A., and Duine, J.A. (1989) Pyrroloquinoline quinone as cofactor in galactose oxidase (EC 1.1.3.9). *J Biol Chem* **264:** 7792–7794.

Munkres, K.D. (1990) Histochemical detection of superoxide radicals and hydrogen peroxide by *Age-1* mutants of *Neurospora. Fung Genet Newslett* **37:** 24–25.

O'Donnell, V.B., and Azzi, A. (1996) High rates of extracellular superoxide generation by cultured human fibroblasts: involvement of a lipid-metabolizing enzyme. *Biochem J* **318** (Pt 3)**:** 805–812.

Picard, M. (1971) Genetic evidence for a polycistronic unit of transcription in the complex locus '14' in *Podospora anserina*. I. Genetic and complementation maps. *Molec Gen Genet* **111:** 35–50.

Rizet, G. (1952) Les phénomènes de barrage chez *Podospora anserina.* I. Analyse génétique des barrages entre souches S and s. *Rev Cytol Biol Veg* **13:** 51–92.

Rizet, G., and Engelmann, C. (1949) Contribution à l'étude génétique d'un Ascomycète tétrasporé: *Podospora anserina* (Ces.) Rehm. *Rev Cytol Biol Veg* **11:** 201–304.

Roy, P., Roy, S.K., Mitra, A., and Kulkarni, A.P. (1994) Superoxide generation by lipoxygenase in the presence of NADH and NADPH. *Biochim Biophys Acta* **1214:** 171–179.

Segmuller, N., Kokkelink, L., Giesbert, S., Odinius, D., van Kan, J., and Tudzynski, P. (2008) NADPH oxidases are involved in differentiation and pathogenicity in *Botrytis cinerea. Mol Plant Microbe Interact* **21:** 808–819.

Semighini, C.P., and Harris, S.D. (2008) Regulation of apical dominance in *Aspergillus nidulans* hyphae by reactive oxygen species. *Genetics* **179:** 1919–1932.

Silar, P. (1995) Two new easy-to-use vectors for transformations. *Fungal Genet Newsl* **42:** 73.

Silar, P. (2005) Peroxide accumulation and cell death in filamentous fungi induced by contact with a contestant. *Mycol Res* **109:** 137–149.

Silar, P., and Picard, M. (1994) Increased longevity of EF-1 alpha high-fidelity mutants in *Podospora anserina. J Mol Biol* **235:** 231–236.

Silar, P., Haedens, V., Rossignol, M., and Lalucque, H. (1999) Propagation of a novel cytoplasmic, infectious and deleterious determinant is controlled by translational accuracy in *Podospora anserina. Genetics* **151:** 87–95.

Stricker, A.R., Mach, R.L., and de Graaff, L.H. (2008) Regulation of transcription of cellulases- and hemicellulases-encoding genes in *Aspergillus niger* and *Hypocrea jecorina* (*Trichoderma reesei*). *Appl Microbiol Biotechnol* **78:** 211–220.

Sumimoto, H. (2008) Structure, regulation and evolution of Nox-family NADPH oxidases that produce reactive oxygen species. *FEBS J* **275:** 3249–3277.

Takemoto, D., Tanaka, A., and Scott, B. (2006) A p67Phox-like regulator is recruited to control hyphal branching in a fungal-grass mutualistic symbiosis. *Plant Cell* **18:** 2807–2821.

Takemoto, D., Tanaka, A., and Scott, B. (2007) NADPH oxidases in fungi: diverse roles of reactive oxygen species in fungal cellular differentiation. *Fung Genet Biol* **44:** 1065–1076.

Tamura, K., Dudley, J., Nei, M., and Kumar, S. (2007) MEGA4: molecular evolutionary genetics analysis (MEGA) software, version 4.0. *Mol Biol Evol* **24:** 1596–1599.

Tanaka, A., Christensen, M.J., Takemoto, D., Park, P., and Scott, B. (2006) Reactive oxygen species play a role in regulating a fungus–perennial ryegrass mutualistic interaction. *Plant Cell* **18:** 1052–1066.

Wesenberg, D., Kyriakides, I., and Agathos, S.N. (2003) White-rot fungi and their enzymes for the treatment of industrial dye effluents. *Biotechnol Adv* **22:** 161–187.

Supporting information

Additional supporting information may be found in the online version of this article.

Please note: Wiley-Blackwell are not responsible for the content or functionality of any supporting materials supplied by the authors. Any queries (other than missing material) should be directed to the corresponding author for the article.